Phase Separation of MAGI2-Mediated Complex Underlies Formation of Slit Diaphragm Complex in Glomerular Filtration Barrier

Haijiao Zhang,[1] Lin Lin,[2] Jianping Liu,[3] Lifeng Pan,[3] Zhijie Lin,[4] Mingjie Zhang,[4,5] Jiong Zhang,[6] Ying Cao,[6] Jinwei Zhu,[2] and Rongguang Zhang[1]

Due to the number of contributing authors, the affiliations are listed at the end of this article.

ABSTRACT

Background Slit diaphragm is a specialized adhesion junction between the opposing podocytes, establishing the final filtration barrier to urinary protein loss. At the cytoplasmic insertion site of each slit diaphragm there is an electron-dense and protein-rich cellular compartment that is essential for slit diaphragm integrity and signal transduction. Mutations in genes that encode components of this membrane-less compartment have been associated with glomerular diseases. However, the molecular mechanism governing formation of compartmentalized slit diaphragm assembly remains elusive.

Methods We systematically investigated the interactions between key components at slit diaphragm, such as MAGI2, Dendrin, and CD2AP, through a combination of biochemical, biophysical, and cell biologic approaches.

Results We demonstrated that MAGI2, a unique MAGUK family scaffold protein at slit diaphragm, can autonomously undergo liquid-liquid phase separation. Multivalent interactions among the MAGI2-Dendrin-CD2AP complex drive the formation of the highly dense slit diaphragm condensates at physiologic conditions. The reconstituted slit diaphragm condensates can effectively recruit Nephrin. A nephrotic syndrome–associated mutation of *MAGI2* interfered with formation of the slit diaphragm condensates, thus leading to impaired enrichment of Nephrin.

Conclusions Key components at slit diaphragm (*e.g.*, MAGI2 and its complex) can spontaneously undergo phase separation. The reconstituted slit diaphragm condensates can be enriched in adhesion molecules and cytoskeletal adaptor proteins. Therefore, the electron-dense slit diaphragm assembly might form via phase separation of core components of the slit diaphragm in podocytes.

JASN 32: 1946–1960, 2021. doi: https://doi.org/10.1681/ASN.2020111590

The glomerular filtration barrier is composed of glomerular endothelial cells, the glomerular basement membrane, and podocytes.[1–3] As the final filtration barrier to urinary protein loss, the slit diaphragm is a highly specialized cell-cell junction formed by the neighboring foot processes of podocytes.[4,5] Disruption of slit diaphragm integrity can lead to various types of nephrotic syndrome defined by severe proteinuria, hypoalbuminemia, and edema.[6,7]

Nephrin, encoded by *NPHS1*, maintains the slit diaphragm structure by forming the specific homotypic *trans*-interactions between the adjacent podocytes.[8] Mutations in *NPHS1* led to the congenital nephrotic syndrome of the Finnish type.[9] Mice lacking *NPHS1* showed alteration of

Received November 12, 2020. Accepted March 22, 2021.

Published online ahead of print. Publication date available at www.jasn.org.

Correspondence: Dr. Jinwei Zhu, Bio-X Institutes, Key Laboratory for the Genetics of Developmental and Neuropsychiatric Disorders, Ministry of Education, Shanghai Jiao Tong University, 1954 Huashan Road, Shanghai 200240, China, or Dr. Rongguang Zhang, State Key Laboratory of Cell Biology, Shanghai Institute of Biochemistry and Cell Biology, Center for Excellence in Molecular Cell Science, Chinese Academy of Sciences, University of Chinese Academy of Sciences, 320 Yueyang Road, Shanghai 200031, China. Email: jinwei.zhu@sjtu.edu.cn or rgzhang@sibcb.ac.cn

slit diaphragm architecture and died perinatally due to massive proteinuria.[10] In addition to the structural role in slit diaphragm assembly, Nephrin plays crucial roles in regulation of actin cytoskeleton dynamics in podocytes. In developing glomeruli, upon phosphorylation, the cytoplasmic tail of Nephrin (Nephrin-CT) binds to adaptor protein Nck, which in turn, recruits proteins associated with actin polymerization (*e.g.*, neuronal Wiskott-Aldrich syndrome protein [N-WASP], actin-related proteins-2/3, *etc.*),[11–13] revealing a physiologic signaling pathway between Nephrin and the actin cytoskeleton in podocytes.[14,15]

In the mature slit diaphragm, Nephrin is linked to the cortical actin cytoskeleton via a multiprotein complex (termed the slit diaphragm complex), which consists of a variety of scaffold proteins and regulatory proteins, including the membrane-associated guanylate kinase (MAGUK) family proteins (*e.g.*, MAGI1, MAGI2, ZO-1, and CASK),[16,17] Podocin,[18] CD2AP (also known as FSGS3),[19] Dendrin,[20] Synaptopodin,[21] α–actinin-4,[16,22] INF2,[23] *etc.* Specifically, Nephrin was reported to bind to MAGI family MAGUKs via its intracellular domain.[16,24,25] MAGI2 binds to Dendrin, whose nuclear translocation has been detected in human glomerular diseases.[20] Dendrin further interacts with CD2AP, a scaffold protein that directly associates with the actin cytoskeleton.[26] Therefore, the slit diaphragm complex (*e.g.*, MAGI2-Dendrin-CD2AP axis) functions as a physical linker between slit diaphragm and actin cytoskeleton and facilitates the Nephrin signaling; the cytoskeleton, in turn, stabilizes Nephrin at the slit diaphragm and ensures the maintenance of the slit diaphragm filter structure.[27,28]

Many mutations that occurred within components of the slit diaphragm complex led to rearrangement of the podocyte cytoskeleton, disruption of the filtration barrier, and subsequent kidney disease.[29,30] For example, *MAGI2* mutations have been identified in patients with steroid-resistant nephrotic syndrome.[31] *MAGI2* whole-knockout mice exhibited a complete disruption of slit diaphragm and died of renal failure.[32,33] Podocyte-specific *MAGI2* knockout mice displayed morphologic defects of podocyte foot processes, disappearance of slit diaphragm, and massive albuminuria.[34] In the absence of MAGI2, Dendrin translocated from slit diaphragm to the nucleus, promoting podocyte apoptosis and glomerulosclerosis.[34] *CD2AP* mutations are associated with sporadic nephritic syndrome and FSGS.[35] *CD2AP* knockout mice developed a congenital nephrotic syndrome with impaired podocyte morphology accompanied by mesangial cell hyperplasia and extracellular matrix deposition and died at 6 weeks of age from kidney failure.[36,37]

Interestingly, biochemical and electron microscopy studies revealed that the cytoplasmic insertion site of each slit diaphragm where the slit diaphragm complex is located is a detergent-resistant, electron-dense region.[38–40] These electron densities contact with the plasma membrane on their one face and with cortical actin cytoskeleton on the other face. Despite the critical roles of the slit diaphragm complex in orchestrating slit diaphragm structure and function, the molecular mechanisms underlying the assembly of the slit diaphragm complex and electron-dense compartment are not well understood.

Significance Statement

Slit diaphragms between podocytes play a critical role in maintaining the filtration function in kidney. At each slit diaphragm there is an electron-dense junctional plaque crucial for slit diaphragm integrity and podocyte signal transduction. However, the molecular basis underlying slit diaphragm assembly is not well understood. Here, we demonstrate that MAGI2, a unique MAGUK family scaffold protein at slit diaphragm, can autonomously undergo liquid-liquid phase separation. Multivalent interactions among the MAGI2-Dendrin-CD2AP complex drive the formation of the slit diaphragm condensates at physiologic conditions. The reconstituted slit diaphragm condensates can effectively enrich Nephrin. A nephrotic syndrome–associated mutation of *MAGI2* interferes with slit diaphragm condensate formation, leading to impaired recruitment of Nephrin. Therefore, the electron-dense slit diaphragm assembly might form via phase separation of the slit diaphragm complex.

In this work, we dissect the interactions of the MAGI2-Dendrin-CD2AP axis and provide the structural basis governing the MAGI2-Dendrin interaction. Importantly, we discover that MAGI2, but not its close paralog MAGI1, undergoes liquid-liquid phase separation (LLPS) both *in vitro* and in living cells. Paralog-specific "RQPPxxxDY" repetitive motifs of MAGI2 are essential for phase separation. More importantly, MAGI2, Dendrin, and CD2AP together form the self-organized, densely packed slit diaphragm condensates, which could effectively recruit Nephrin. A nephrotic syndrome–associated mutation of MAGI2 impairs the formation of the slit diaphragm condensates, thus leading to defects of Nephrin recruitment.

METHODS

Constructs and Peptides

Mouse *MAGI1* (GenBank: NM_001286784.1), *MAGI2* (GenBank: NM_001170746.1), *Dendrin* (GenBank: NM_001013741.1), and *Nephrin* (GenBank: NM_019459.2) genes were amplified from a mouse brain cDNA library. Human *CD2AP* (GenBank: NM_012120.3) and *MAGI3* (NM_001142782.2) were provided by Jiahuai Han (Xiamen University, China). Various fragments of these genes were amplified by standard PCR method and cloned into pGEX-4T-1, pET32M-3C, pEGFP-C, pEBFP-C, pTRFP, or pcDNA3.0-FLAG vector. Mutations were created through site-directed mutagenesis method and confirmed by DNA sequencing.

All peptides were commercially synthesized by Genscript (China) with purity >95%.

Protein Expression and Purification

Wild-type or various mutants of MAGI2 and CD2AP were expressed in BL21(DE3) and Rosetta (DE3) cells,

respectively, at 20°C for 20 hours induced by 0.4 mM isopropyl-β-D-thiogalactoside (IPTG). Trx-His_6–tagged Nephrin-CT was expressed in BL21(DE3) cells at 37°C for 2.5 hours induced by 0.4–0.6 mM IPTG. The Dendrin protein was expressed in BL21(DE3) cells at 30°C for 4 hours induced by 0.4 mM IPTG. Other constructs were expressed in BL21(DE3) cells at 16°C for 20 hours induced by 0.2 mM IPTG. His_6-tagged and GST-tagged proteins were purified by Ni^{2+}-NTA agarose affinity chromatography and GSH-Sepharose affinity chromatography, respectively, followed by a Superdex-200 26/60 size-exclusion chromatography (SEC) in the buffer containing 50 mM Tris, pH 8.0, 100 mM NaCl, 1 mM EDTA, 1 mM dithiothreitol (DTT), and protease inhibitor cocktail. His_6 tag was then removed by addition of human rhinovirus 3C proteinase at 4°C overnight, followed by another round of SEC.

Isothermal Titration Calorimetry Assay

Isothermal titration calorimetry assays were carried out to measure the binding affinity of various interactions. All of the measurements were performed at 25°C using a MicroCal iTC200 system (Malvern). Dendrin peptides (the concentrations ranging from 100 to 300 μM) or δ-catenin PDZ-binding motif (PBM) peptide (500 μM) was in the syringe. MAGI2 WW1–2 (10 μM), PDZ5 (50 μM), or PDZ5–8RA (50 μM) was in the cell. All of the samples were in the buffer containing 50 mM Tris, pH 8.0, 100 mM NaCl, 1 mM EDTA, and 1 mM DTT. The data were analyzed using the ORIGIN 7.0 software (MicroCal Software).

Fluorescence Polarization Assay

To determine the binding affinities between the SH3 domains of CD2AP and proline-rich regions (*i.e.*, PRn and PRc) of Dendrin, the fluorescence polarization assay was performed on a PerkinElmer LS-55 fluorimeter at 25°C. The commercially synthesized peptides of PRn and PRc were labeled with FITC (Invitrogen; Molecular Probe) in the buffer containing 0.1 M $NaHCO_3$ at room temperature for 1 hour and then exchanged into the buffer containing 50 mM Tris, pH 8.0, 100 mM NaCl, 1 mM EDTA, and 1 mM DTT. The FITC-labeled PRn and PRc peptides were titrated with the SH3 domains of CD2AP. The K_d value was fitted with the classic one-site binding model using GraphPad Prism 7.

GST–Pull-Down Assay

Flag-tagged full-length MAGI2 was overexpressed in HEK293T cells. Cells were harvested and lysed using the ice-cold cell lysis buffer containing 50 mM HEPES, pH 7.4, 150 mM NaCl, 10% glycerol, 2 mM $MgCl_2$, 1% Triton, and protease inhibitor cocktail. After centrifugation, the supernatants were incubated with 20 μl various wild-type or mutants of GST-Nephrin fragments preloaded GSH-Sepharose 4B slurry beads. After extensive washing with the cell lysis buffer, the captured proteins were eluted by 30 μl 2× SDS-PAGE loading dye and detected by western blot using anti-Flag antibody (Sigma-Aldrich; 1:3000, catalog no. F1804).

Crystallography

For the reconstitution of the MAGI2 WW1–2/Dendrin PY2–3-Ex (amino acids 222–241) complex, Trx-His_6–tagged MAGI2 WW1–2 was copurified with Trx-His_6–tagged Dendrin PY2–3-Ex. The Trx-His_6 tag was removed by incubation with human rhinovirus 3C protease overnight, followed by another round of SEC.

The best crystals of the complex (approximately 15 mg/mL) were obtained by the sitting-drop vapor diffusion method at 16°C in 2.2 M ammonium sulfate, 150 mM malate, pH 5.1, and 4.0% (vol/vol) 1,2-propanediol. Crystals were soaked in 4 M ammonium sulfate for cryoprotection. The x-ray diffraction data were collected at 100 K at the Shanghai Synchrotron Radiation Facility. The diffraction data were processed with the HKL3000 package.[41] The complex structure was solved by molecular replacement by PHASER[42] using the structures of MAGI1-WW1 (Protein Data Bank [PDB]: 2YSD) and MAGI1-WW2 (PDB: 2YSE) as the searching models. The refinement was carried out using the programs PHENIX[43] and COOT.[44] The final processing and refinement statistics of the complex structure are listed in Supplemental Table 1. All structural diagrams were prepared using PyMOL.

Fast Protein Liquid Chromatography Coupled with Static Light Scattering

The molecular weight analysis was carried out by the Agilent InfinityLab system coupled with a static light scattering detector (miniDawn; Wyatt) and a differential refractive index detector (Optilab; Wyatt). One hundred microliters of CD2AP-CC or CD2AP-CC^{LK} at the concentration of 100 μM was loaded into a Superose 12 10/300 GL column (GE Healthcare) pre-equilibrated with 50 mM Tris, pH 8.0, 100 mM NaCl, 1 mM EDTA, and 1 mM DTT buffer. Data were analyzed using ASTRA 6 software (Wyatt).

Protein Labeling with Fluorophore

The proteins for labeling were exchanged into buffer containing 100 mM NaCl, 100 mM $NaHCO_3$, pH 8.3, and 4 mM β-ME using a HiTrap desalting column with the concentration of approximately 5 mg/ml. iFluor 405 ester (AAT Bioquest), Cy3/Cy5 NHS ester (AAT Bioquest), and Alexa 488 NHS ester (Thermo Fisher) were dissolved in DMSO and were incubated with the protein at room temperate for 1 hour. The label reaction was quenched by the addition of the buffer containing 50 mM Tris, pH 8.0, 100 mM NaCl, 1 mM EDTA, and 1 mM DTT. The labeled protein was separated with a HiTrap desalting column to remove excess dye into the same buffer. Fluorescence labeling efficiency was measured by Nanodrop 2000 (Thermo Fisher).

In Vitro Phase Separation Assay

Freshly purified proteins were dissolved in the buffer containing 50 mM Tris, pH 8.0, 100 mM NaCl, 1 mM EDTA, and 1 mM DTT and then centrifuged at 14,000 rpm for 10 minutes at 4°C. Subsequently, all of the samples were placed on ice before phase separation assay.

For the sedimentation-based assay, proteins or protein complex mixtures were centrifuged at 14,000 rpm for 5 minutes at room temperature. Samples from the supernatant and pellet fraction were analyzed by SDS-PAGE. The intensity of each band was quantified by ImageJ and GraphPad Prism 7. Each group was repeated three times. Data were presented as mean ± SD. For the microscope-based assay, each sample (labeled proteins or complex mixtures) was injected in a chamber described previously for fluorescent imaging (Leica SP8).

Fluorescence Recovery after Photobleaching Assay

GFP-tagged full-length MAGI2 or CD2AP was expressed in COS7 cells, which were cultured on glass-bottom dishes (MatTek) for *in vivo* fluorescence recovery after photobleaching (FRAP) assay. The FRAP assays were carried out on a Leica SP8 confocal microscope with a 63× oil objective, and GFP signal was bleached with a 488-nm laser beam. The ROI intensity at the time right after the photobleaching was set as 0%, and the prebleaching intensity was normalized to 100%.

Nuclear Magnetic Resonance Spectroscopy

The labeled proteins for nuclear magnetic resonance studies were concentrated to approximately 0.3 mM in a buffer containing 50 mM NaH_2PO_4/Na_2HPO_4, pH 7.0, 50 mM NaCl, 10% D_2O (vol/vol), and 1 mM DTT. ^{1}H-^{15}N HSQC spectra were acquired at 25°C on an Agilent 800-MHz spectrometer (Agilent Technology). Peptide (P1: PKKPPPP) was dissolved in the same buffer and titrated into the three SH3 domains of CD2AP with indicated molar ratio.

Cellular Localization Assay

HEK293T cells were plated on glass coverslips and transfected with the indicated plasmids using a Lipofectamine-2000 Reagent (Invitrogen; Thermo Fisher Scientific). Cells were cultured in DMEM containing 10% FBS in 5% CO_2 before fixation. After transfection for 20 hours, cells were fixed with 4% paraformaldehyde for 15 minutes at room temperature. After three times washing with PBS, cells were mounted on glass slides with Vectashield Mounting Medium (Axxora) for image acquisition on the Olympus IX71 inverted fluorescent microscope.

Quantification and Statistical Analyses

Statistical parameters, including the definitions and exact values of *n* (*e.g.*, the number of experiments), are described in the figures. For the sedimentation-based assay and the percentage of cells displaying spherical puncta, all data are expressed as mean ± SD. Statistical analysis was performed by GraphPad Prism 7.

RESULTS

MAGI2 Undergoes Phase Separation *In Vitro* and in Living Cells

We previously uncovered the structural basis of the specific interaction between the evolutionarily conserved atypical PBM of Nephrin and PDZ3 domain of MAGI1.[45] During our further study of the interaction between Nephrin and MAGI2, we came across an interesting discovery that GFP-MAGI2 forms spherical puncta under fluorescence microscopy when expressed in a fibroblast kidney cell line, COS7 cells (Figure 1A). To figure out whether the GFP-MAGI2 puncta are irreversible aggregates or reversible condensed droplets, we performed the FRAP experiment. The FRAP assay showed that GFP-MAGI2 signal could be recovered after photobleaching over a short period of time, suggesting that GFP-MAGI2 could rapidly exchange between the puncta and the surrounding dilute cytoplasm (Figure 1, A and B). We next purified the recombinant full-length MAGI2 protein and labeled the protein with Alexa 488 fluorophore. Alexa 488-MAGI2 formed spherical droplets in a concentration-dependent manner under microscopy (Figure 1C). These dispersed droplets could fuse with each other over time (Figure 1D). To investigate the biophysical properties of these condensed droplets, we test their ability to form droplets under different salt concentrations. We found that the size of the MAGI2 droplets was reduced with elevated salt concentration (Figure 1E). These above features are characteristic of phase-separated biomolecular condensates,[46–48] suggesting that MAGI2 may autonomously undergo LLPS *in vitro* and in living cells.

Molecular Mechanism Governing the Phase Separation of MAGI2

In general, the biomolecular condensates are driven by multivalent intra- or intermolecular interactions either between multidomain scaffold proteins (*e.g.*, tandem SH3 domains and proline-rich motifs)[47] or between low-complexity sequences of intrinsically disordered regions (*e.g.*, fused in sarcoma [FUS]).[49] MAGI2 belongs to the MAGUK family protein and contains six PDZ domains, two WW domains, and a guanylate kinase–like (GK) domain (Figure 2A). To the best of our knowledge, there are no intra- or intermolecular interactions between these domains; MAGI2 lacks the intrinsically disordered regions with high disorder tendency according to the prediction program IUpred.[50]

To uncover the mechanism governing the phase separation of MAGI2, we purified various truncation or deletion forms of MAGI2 and tested their abilities to form the condensed droplets. We found that deletion of PDZ0-GK,

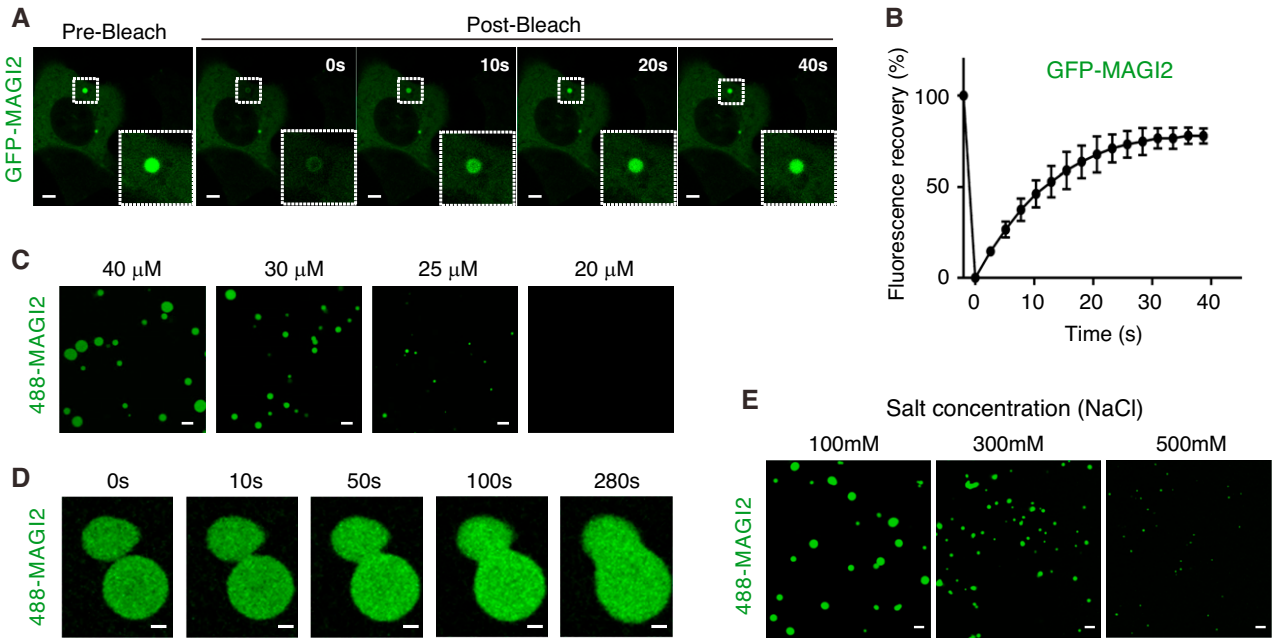

Figure 1. MAGI2 undergoes phase separation *in vitro* and in living cells. (A) Representative images show that expression of GFP-MAGI2 in COS7 cells produced many bright and spherical puncta. Representative time-lapse FRAP images show that the GFP-MAGI2 signal within the puncta recovered over a short period of time. Show the enlarged images of MAGI2 droplets selected for FRAP experiment. Scale bars: 5 μm. (B) Quantitative results for FRAP analysis of GFP-MAGI2 in puncta of COS7 cells. The curve represented the averaged signals from ten droplets. Time 0 refers to the time point of the photobleaching pulse. All data are represented as mean ± SD. (C) Fluorescence images showing that purified MAGI2 protein underwent phase separation at indicated concentrations. The images were acquired at room temperature with 1% MAGI2 labeled by Alexa 488. The protein labeling ratio and the imaging conditions were used throughout the study unless otherwise stated. Scale bars: 5 μm. (D) Representative images showing that the MAGI2 condensed droplets fused with each other over time. Scale bars: 1 μm. (E) Phase separation of MAGI2 in the presence of different salt conditions. Scale bars: 5 μm.

PDZ3, or PDZ5 significantly disrupted phase separation, whereas deletion of WW1–2, PDZ1, PDZ2, or PDZ4 had no effect (Figure 2, A and B). A characteristic hallmark of PDZ0-GK, PDZ3, and PDZ5 domains is that they are all enriched with arginine (Arg, R) residues (PDZ0-GK: 10R; PDZ3: 14R; PDZ5: 12R) (Figure 2A). Interestingly, this feature is highly conserved in MAGI2 from different species and among three paralogs of MAGI family proteins (MAGI1–3) (Supplemental Figure 1). We first wanted to investigate whether reduced arginine content of the arginine-rich domains in MAGI2 will impair the phase separation. We chose to replace eight of 12 arginine residues in the PDZ5 domain with alanine residues (referred to as MAGI2$^{PDZ5-8RA}$ mutant) (Figure 2A, Supplemental Figure 2). Notably, most of the arginine residues chosen for substitution are located at the loop regions of PDZ5 (Supplemental Figure 2); the PDZ5–8RA mutant displayed a similar binding ability to δ-catenin PBM peptide as the wild-type PDZ5 did (Supplemental Figure 2), suggesting that alanine substitution did not change the overall folding of MAGI2 PDZ5. Intriguingly, MAGI2$^{PDZ5-8RA}$ lost its ability to form phase separation (Figure 2B), implying that the arginine content of the arginine-rich domains of MAGI2 is indeed critical for its phase separation.

However, the fact that MAGI1 did not form phase-separated droplets (see below for detail) led us to speculate that some paralog-specific regions of MAGI2 other than these arginine-rich domains may also contribute to the phase separation. Careful sequence analysis indicated that a unique loop between PDZ4 and PDZ5 domains of MAGI2, which comprises several "RQPPxxxDY" repetitive motifs (referred to as the "DY loop" hereafter), is absent in MAGI1 and MAGI3 (Figure 2C). We replaced all of the tyrosine residues in the DY loop with serine residues (referred to as the MAGI2^{YS} mutant) (Figure 2C) and found that the MAGI2^{YS} mutant failed to form condensed droplets even at the concentration above 80 μM (Figure 2B). It is worth noting that the DY loop is conserved in MAGI2 from human to fish, whereas *Caenorhabditis elegans* MAGI lacks the DY loop (Figure 2C). Consistent with this analysis, zebrafish MAGI2 also formed phase-separated droplets, whereas *C. elegans* MAGI did not (Figure 2D). Furthermore, we designed a chimeric construct where the DY loop of mouse MAGI2 is inserted between PDZ4 and PDZ5 domains of mouse MAGI1. Interestingly, the mouse MAGI1_DY chimeric construct gained the ability to form phase separation (Figure 2D), indicating the indispensable role of the DY loop for phase separation.

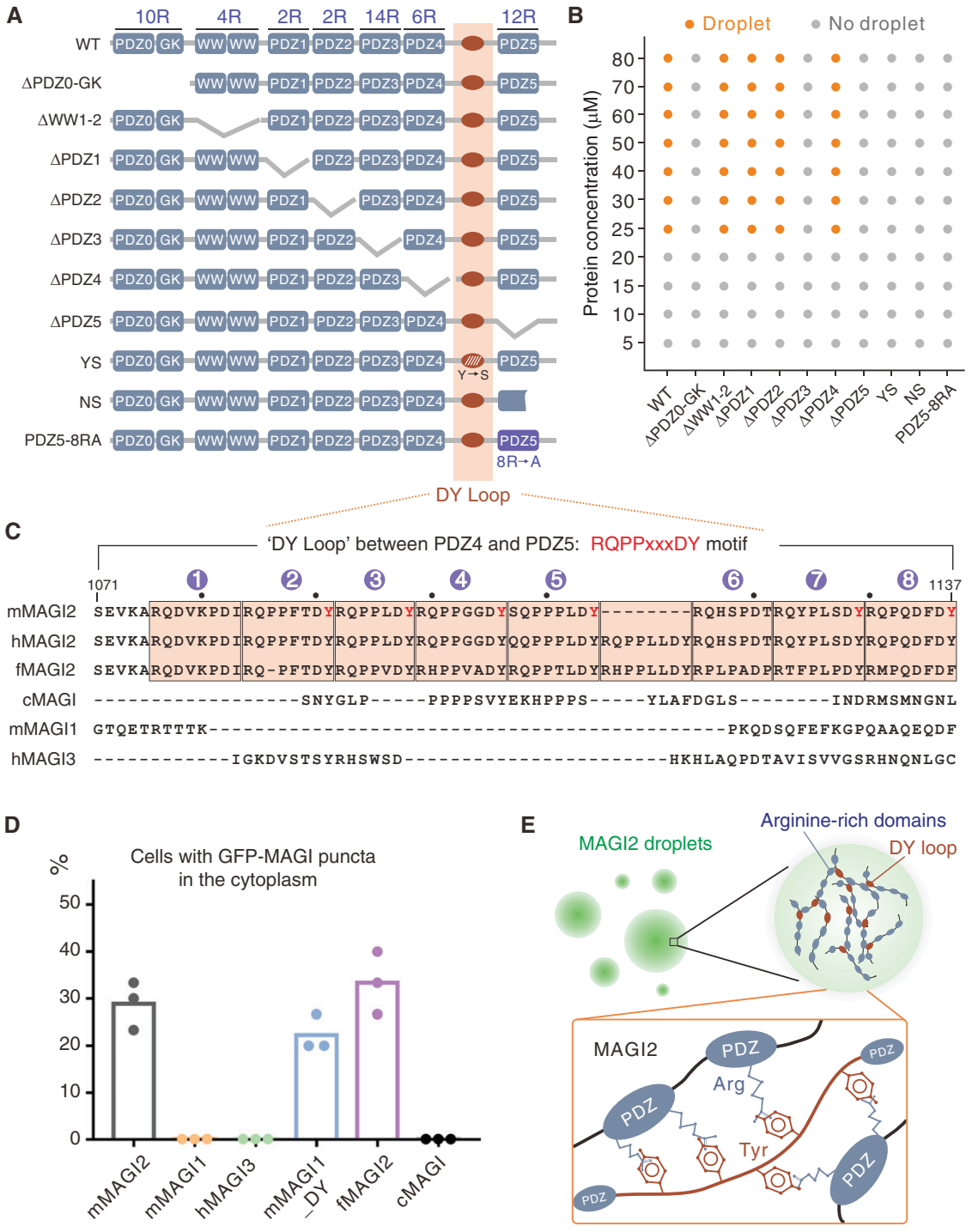

Figure 2. Molecular mechanism governing the phase separation of MAGI2. (A) Schematic diagrams showing the domain organizations of various fragments of MAGI2. The DY loop between PDZ4 and PDZ5 domains is highlighted with an orange box. The arginine content of each domain is also shown. (B) Phase separation diagram of wild-type (WT) and mutant forms of MAGI2 at indicated concentrations. The highlighted orange dots indicate phase separation (phase separation happens at this concentration); the gray dots indicate that there is no phase separation (phase separation does not happen at this concentration). (C) Sequence alignment of the DY loop between PDZ4 and PDZ5 domains. Note that mouse MAGI2 contains several "RQPPxxxDY" repetitive motifs. c, *C. elegans*; f, zebrafish; h, human; m, mouse. (D) The percentage of cells showing spherical MAGI puncta. All data are expressed as mean ± SD (n=3; number of batches of cultures with 30 cells counted for each batch). (E) Hierarchical organization of the formation of condensates is depicted here as spherical droplets showing that collective interactions between tyrosine residues in the DY loop and arginine residues in PDZ domains of MAGI2 are the major driving force for phase separation.

Taken together, these results suggested that phase separation of MAGI2 is governed by multivalent interactions between the tyrosine residues from the paralog-specific "RQPPxxxDY" repetitive motifs and the arginine residues from surfaces of PDZ domains (Figure 2E). This mechanism resembles the one utilized by FUS protein. However, unlike FUS phase separation where the arginine residues are from the low–sequence complexity region,[51] the arginine residues required for MAGI2 phase separation are situated at the solvent-exposed surfaces of well-folded PDZ domains. Therefore, when searching for proteins capable of undergoing phase separation, one will need to pay attentions to arginine-rich motifs not only in the unstructured intrinsic disorder region(s) but also, in the solvent-exposed surfaces of folded domain(s).

Notably, a protein-truncating mutation (p.E1178Dfs×9) of MAGI2 ($MAGI2^{NS}$) was identified in patients with steroid-resistant nephrotic syndrome.[31] This mutant protein is expected to disrupt the PDZ5 domain of MAGI2 (Supplemental Figure 3). Because PDZ5 is required for MAGI2 phase separation, the $MAGI2^{NS}$ mutant failed to form phase-separated droplets as expected (Figure 2B).

Biochemical and Structural Characterization of MAGI2-Dendrin Interaction

We next wanted to know whether MAGI2-mediated slit diaphragm complex (*e.g.*, MAGI2-Dendrin-CD2AP) shows the similar biophysical features as phase-separated MAGI2 does. MAGI2 interacts with Dendrin in glomeruli, which play an important role in sequestering Dendrin at the slit diaphragm.[34] The interaction is mediated by WW1–2 tandem of MAGI2 and the PPxY motifs of Dendrin (Figure 3A). Dendrin contains three PPxY motifs (PY1–3) (Figure 3B). Notably, PY2 and PY3 are connected by only two residues, whereas PY1 is far away from PY2–3 (Figure 3B). The isothermal titration calorimetry–based assay showed that MAGI2 WW1–2 binds to PY1 with a dissociation constant (K_d) of approximately 4 μM (Figure 3C). In contrast, PY2–3 bound to MAGI2 WW1–2 with an approximately 300-fold higher affinity than PY1 did (K_d∼0.013 μM) (Figure 3C). More interestingly, extension of eight residues following PY2–3 (referred to as PY2–3-Ex) further enhanced the binding affinity by approximately four-fold (K_d∼0.003 μM) (Figure 3C).

We solved the crystal structure of MAGI2 WW1–2 in complex with Dendrin PY2–3-Ex at 2.1-Å resolution (Supplemental Table 1). In the complex structure, Dendrin PY2–3-Ex binds to MAGI2 WW1–2 in an antiparallel manner, with WW1 bound to PY3 and WW2 bound to PY2 (Figure 3D). The eight–amino acid Ex fragment contacts with the side of WW1 (Figure 3D). Specifically, P224/P225 of PY2 and P230/P231 of PY3 form hydrophobic contacts with Y364/F375 of WW2 and Y318/W329 of WW1, respectively (Figure 3D). Y227 of PY2 and Y233 of PY3 form hydrogen bonds with H368 of WW2 and H322 of WW1, respectively. These interaction details represent the typical PPxY-WW interaction mode.[52,53] As expected, mutation of the three tyrosine residues from PY1–3 to alanine (*i.e.*, $Dendrin^{YA}$) completely disrupted the MAGI2-Dendrin interaction (Supplemental Figure 4). Notably, the side chain of $H237^{Dendrin}$ from the eight–amino acid Ex fragment forms a hydrogen network with the side chain of $Y318^{WW1}$ and the main chain of $Y233^{Dendrin}$ (Figure 3D). Substitution of H237 with alanine in PY2–3-Ex decreased the binding affinity by approximately four-fold (K_d∼0.013 μM), revealing the importance of $H237^{Dendrin}$-mediated hydrogen bond interactions for the intact MAGI2-Dendrin interaction.

Interaction between Dendrin and CD2AP

Dendrin was shown to bind directly to CD2AP in the podocytes.[20] Moreover, a proline-rich fragment C terminal to the PPxY motifs of Dendrin (amino acids: RPVPRSRQHLR, referred to as "PRc") was shown to bind to the second SH3 domain of CIN85, a close homolog of CD2AP.[54] CD2AP contains three SH3 domains (SH3a–c). We set out to test the binding of Dendrin PRc to each SH3 domain of CD2AP using fluorescence spectroscopy. Dendrin PRc bound to SH3a, SH3b, and SH3c domains of CD2AP with K_d values of 96, 38, and 878 μM, respectively (Figure 3E). Intriguingly, we found that another proline-rich sequence preceding the PPxY motifs of Dendrin (amino acids: QPRPEPRNALR, referred to as "PRn") also fits well with the reported consensus motif required for CIN85 SH3 binding[54] (Figure 3E). As expected, Dendrin PRn bound to each SH3 domain of CD2AP, although the binding affinities were much lower than those of PRc-SH3 interactions (Figure 3E). In line with the fact that R(0) is critical for CIN85 SH3-PR motif interaction,[54] substitution of the corresponding arginine in PRn and PRc of Dendrin with Glu (*i.e.*, PRn^{RE} and PRc^{RE}) significantly impaired their bindings to CD2AP and SH3b, respectively (Supplemental Figure 4).

Multivalent Protein-Protein Interactions Drive the Slit Diaphragm Condensates Formation

Because both of the PY1 and PY2–3 motifs of Dendrin are capable of binding to MAGI2 WW1–2, one can envision that binding of Dendrin to MAGI2 would expand the valency of the system and thus, promote the phase separation of MAGI2. Moreover, two PR motifs of Dendrin bind to each SH3 domain of CD2AP. Therefore, addition of CD2AP into the MAGI2-Dendrin complex might further expand the valency and facilitate the slit diaphragm condensates formation. To test our hypothesis, we wanted to purify full-length Dendrin and CD2AP proteins and investigate their effects on MAGI2 phase separation. Although we can get purified full-length CD2AP protein, we failed to get full-length Dendrin protein. Instead, we purified a truncated Dendrin protein,

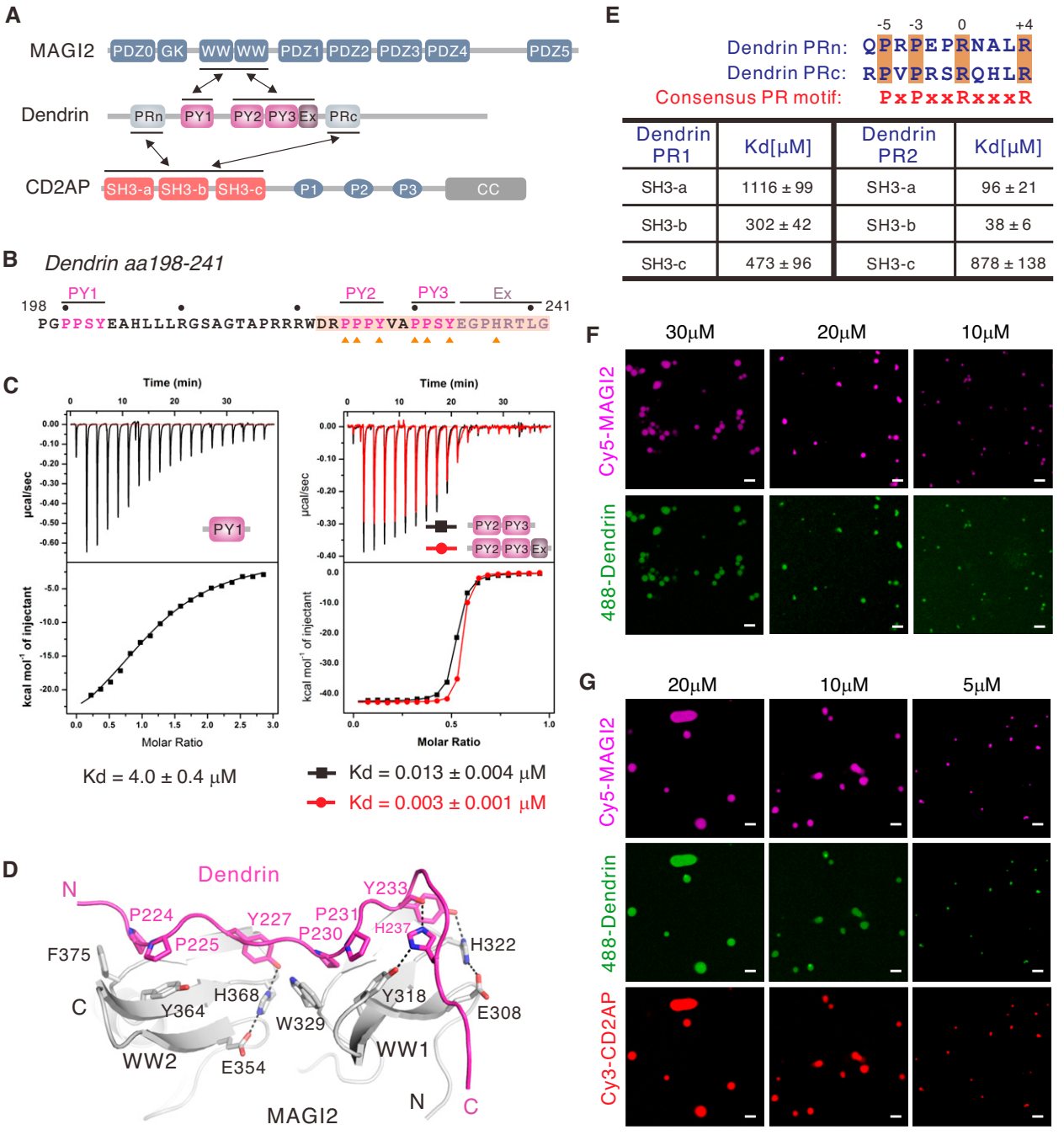

Dendrin PR1	Kd[μM]	Dendrin PR2	Kd[μM]
SH3-a	1116 ± 99	SH3-a	96 ± 21
SH3-b	302 ± 42	SH3-b	38 ± 6
SH3-c	473 ± 96	SH3-c	878 ± 138

Figure 3. MAGI2, Dendrin, and CD2AP together form the slit diaphragm condensates. (A) Schematic diagrams showing the domain organizations of MAGI2, Dendrin, and CD2AP. The interactions among these proteins are indicated by the two-way arrows. (B) Amino acid sequence of Dendrin 198–241. Three PPxY motifs are colored purple. The fragment used for crystallography study is highlighted with the yellow-orange box. Residues involved in binding to WW1–2 are annotated below as orange triangles. (C) The isothermal titration calorimetry curves showing the bindings of WW1–2 to PY1, PY2–3, and PY2–3-Ex. (D) Detailed interface between WW1–2 and PY2–3-Ex. Hydrogen bonds are shown as black dashed lines. (E) Summary of binding affinities derived from the fluorescence polarization–based assays between two PR motifs of Dendrin and three SH3 domains of CD2AP. The consensus SH3-binding motif (*i.e.*, PxPxxRxxxR) of CIN85 or CD2AP is also shown. (F) Fluorescence images showing that the mixture of MAGI2 and Dendrin led to phase separation at the indicated concentrations. MAGI2 and Dendrin were labeled with Cy5 and Alexa 488, respectively. Scale bars: 5 μm. (G) Fluorescence images showing that the mixture of MAGI2, Dendrin, and CD2AP at indicated concentrations resulted in condensed droplets with three components codroplet with each other. MAGI2, Dendrin, and CD2AP were labeled with Cy5, Alexa 488, and Cy3, respectively. Scale bars: 5 μm.

which includes two PR motifs (for CD2AP binding) and three PPxY motifs (for MAGI2 binding), as this protein behaves well and is suitable for phase separation study. For simplicity, we refer to this protein as Dendrin here.

We found that mixing equal amounts of Cy5-labeled MAGI2 and Alexa 488–labeled Dendrin led to formation of the condensed liquid droplets (Figure 3F). Notably, addition of Dendrin lowered the threshold concentration for MAGI2 to undergo phase separation (Figure 3F, 10 μM versus Figure 1C, 25 μM). However, Dendrin alone did not form phase separation even at the concentration of 100 μM (data not shown). Moreover, RFP-Dendrin colocalized with GFP-MAGI2 in the spherical puncta when they were coexpressed in COS7 cells, whereas no puncta were observed in cells that expressed RFP-Dendrin alone (Supplemental Figure 5). These data suggested that binding of Dendrin promotes the phase separation of MAGI2. Addition of CD2AP into the MAGI2-Dendrin mixture further lowered the threshold concentration of phase separation (Figure 3G, 5 μM versus Figure 3F, 10 μM). It is worth noting that the slit diaphragm condensates formed by the MAGI2-Dendrin-CD2AP complex were readily observed at an individual protein concentration of 5 μM (Figure 3G). As expected, MAGI2-Dendrin-CD2AP complex can spontaneously form phase-separated droplets when coexpressed in COS7 cells (Supplemental Figure 5).

CD2AP Undergoes Liquid-Liquid Phase Transition

During our study of the slit diaphragm condensates, we found that purified CD2AP protein alone forms condensed droplets in a concentration-dependent manner (Figure 4A). GFP-CD2AP was observed to form spherical puncta when expressed in COS7 cells (Figure 4B). The FRAP assay showed that GFP-CD2AP signal could be recovered rapidly after photobleaching (Figure 4C). These data indicated that CD2AP also undergoes LLPS.

A series of CD2AP constructs was generated to test their abilities to form droplets *in vitro* (Figure 4D). Deletion of three SH3 domains, the coiled coil (CC) domain, or the linker region abrogated the droplets formation (Figure 4, D and E). Similar to its homolog CIN85, CD2AP-CC is a trimer in solution (Supplemental Figure 6). On the basis of the structure of CIN85-CC,[55] we designed a two-point mutation of CD2AP-CC (*i.e.*, L539K/L625K double mutation; referred to as the "LK" mutant) capable of converting trimeric CD2AP-CC into a monomer (Supplemental Figure 6). The $CD2AP^{LK}$ mutant did not form phase-separated droplets, further confirming that CC-mediated oligomerization is required for phase separation. We further deleted the three specific proline-rich motifs (P1–3) and found that this mutant also lost its phase separation ability (Figure 4, D and E). We hypothesized that multivalent interactions between P1–3 motifs and SH3a–c domains might be required for CD2AP phase transition. We chose P1 motif to titrate with each SH3 domain of CD2AP using a nuclear magnetic resonance–based titration assay. Three SH3 domains all bound specifically to P1 motif (Supplemental Figure 7). Because P1–3 motifs are highly similar with each other, we believe that P2 and P3 can both bind to SH3 domains of CD2AP as well. Thus, we concluded that the CC domain and the multivalent interactions between the P1–3 motifs and SH3 domains of CD2AP are both required for CD2AP phase separation (Figure 4F).

The Slit Diaphragm Condensates Recruit Nephrin

The most pivotal role of the slit diaphragm complex is to connect Nephrin with cortical actin cytoskeleton in the foot processes of podocytes, thus maintaining the integrity of mature slit diaphragm. Nephrin was shown to directly bind to MAGI2 in glomeruli.[16,25] Although the conserved PBM of Nephrin bound weakly to MAGI2,[45] the entire Nephrin-CT bound to MAGI2 more robustly (Figure 5, A and B). Notably, Nephrin-CT without PBM completely lost the ability to bind to MAGI2 (Figure 5B). These data indicated that both the PBM of Nephrin and its upstream sequence are required for the intact MAGI2-Nephrin interaction. A very recent study has shown that PDZ3–5 domains of MAGI2 are required for Nephrin binding.[25] Further structural investigation is need to illustrate the interaction detail in future.

We next wanted to test whether the slit diaphragm scaffold condensates could incorporate Nephrin-CT. We purified and labeled the Nephrin-CT with iFluor 405 fluorophore and mixed it with Cy5-MAGI2, 488-Dendrin, and Cy3-CD2AP. The resulting four-component mixture underwent LLPS even at the concentration of 1 μM (Figure 5C, Supplemental Figure 8), implying that the condensates might form at the physiologic condition in podocytes. The distribution of four proteins between the bulk aqueous solutions (the "supernatant" faction) and the condensed droplets (the "pellet" fraction) was analyzed by a sedimentation-based assay described previously.[56] At the concentration of 10 μM, approximately 70% of MAGI2, approximately 80% of CD2AP, approximately 70% of Dendrin, and approximately 45% of Nephrin-CT proteins were recovered from the condensed phase (Figure 5, D and E). However, both the $Dendrin^{YA}$ mutant (defective in formation of the MAGI2-Dendrin complex) and the $Dendrin^{RE}$ mutant (defective in formation of the Dendrin-CD2AP complex) showed impairment in forming the slit diaphragm condensates and reduced Nephrin-CT recruitment to the condensates (Figure 5, D and E). Moreover, the nephrotic syndrome–associated mutant of MAGI2, $MAGI2^{NS}$, also resulted in reduced Nephrin-CT recruitment (Figure 5, D and E). Because $MAGI2^{NS}$ displayed a similar binding ability to Nephrin-CT as the wild-type MAGI2 did (Supplemental Figure 9), the reduced Nephrin-CT recruitment was most likely due to the attenuated slit diaphragm condensates formed by the $MAGI2^{NS}$ mutant.

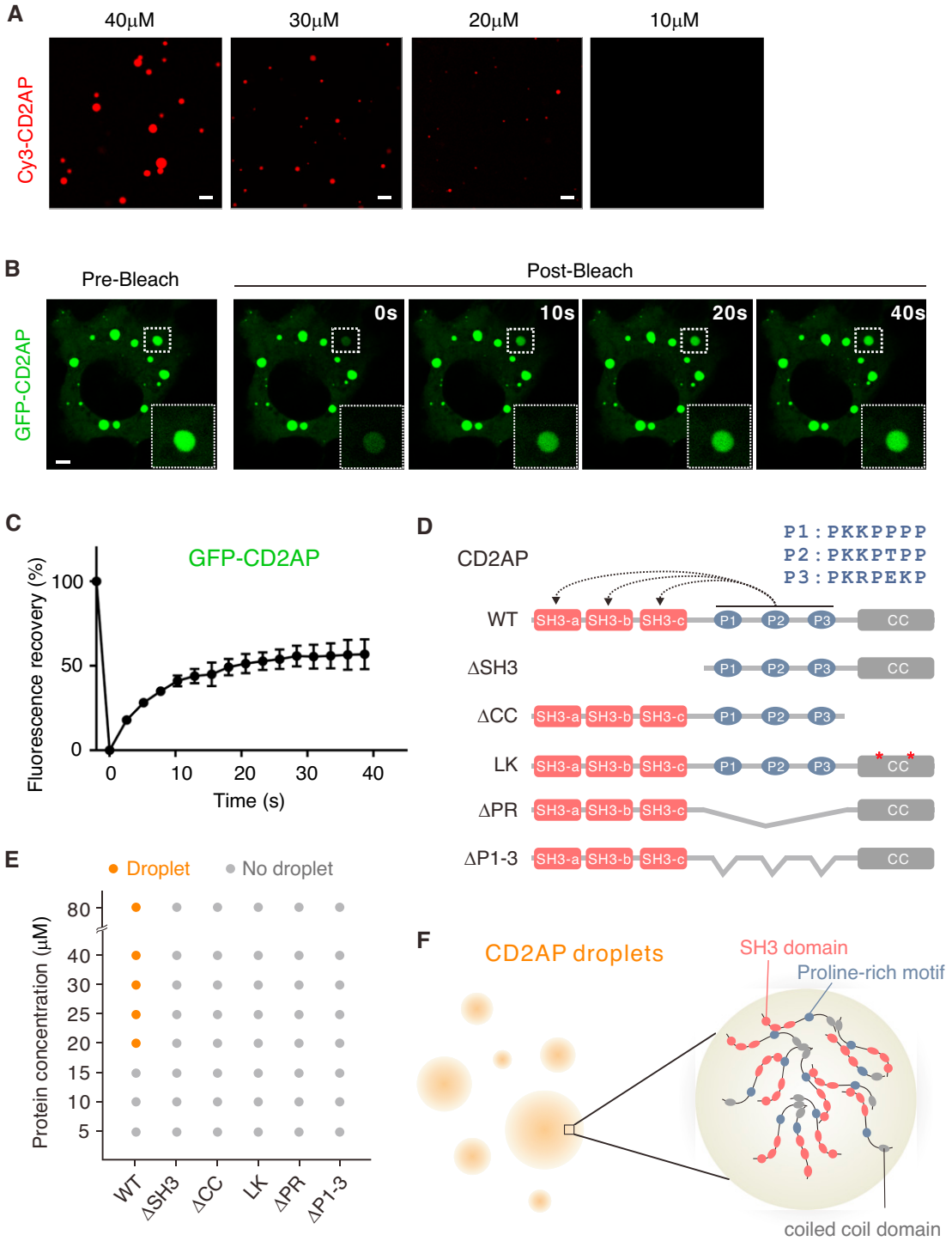

Figure 4. CD2AP forms phase transition *in vitro* and in living cells. (A) Fluorescence images show that purified CD2AP protein underwent phase separation at indicated concentrations. Scale bars: 5 μm. (B) Representative images show that the expression of GFP-CD2AP in COS7 cells generated bright and spherical puncta. FRAP experiment shows that the GFP-CD2AP signal within the puncta recovered over time. Show the enlarged images of CD2AP droplets selected for FRAP experiment. Scale bar: 5 μm. (C) Quantitative results for FRAP analysis of GFP-CD2AP in puncta of COS7 cells. The curve represents the averaged signals from ten droplets. All data are represented as mean ± SD. (D) Schematic diagrams showing the domain organizations of various truncations of CD2AP. The amino acid sequences of three proline-rich sequences in the linker region (P1–P3) are shown. The interactions between SH3 domains and proline-rich sequences are indicated with dashed arrows. (E) Phase separation diagram of wild-type (WT) and mutant forms of CD2AP at indicated concentrations. The highlighted orange dots indicate phase separation; gray dots indicate no phase separation. (F) A model depicting the mechanism of CD2AP phase separation.

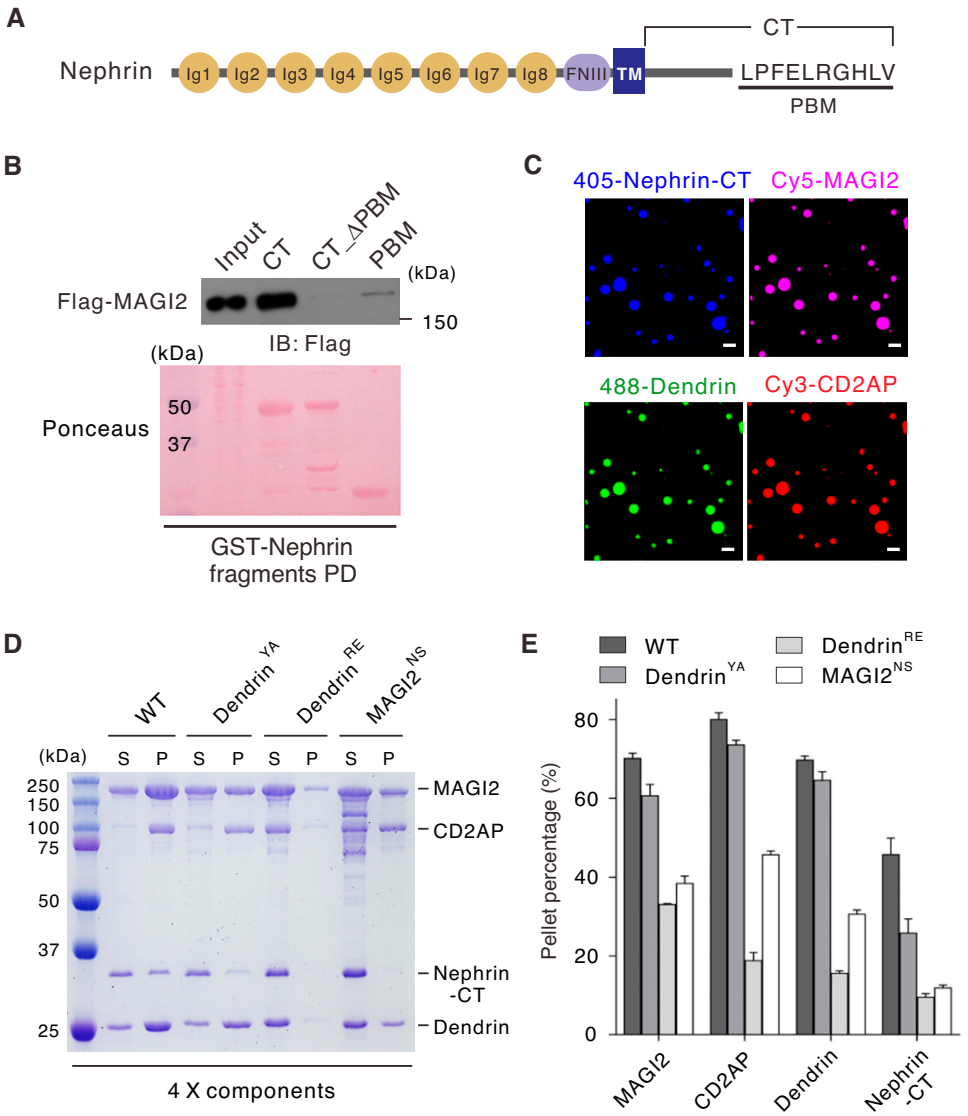

Figure 5. The slit diaphragm condensates effectively recruit Nephrin. (A) Domain organization of Nephrin. Sequence of Nephrin-PBM (-LPFELRGHLV) is shown. CT, cytoplasmic tail. (B) GST–pull-down analysis of the interactions between various fragments of Nephrin and Flag-tagged full-length MAGI2 expressed in HEK293T cells. (C) Fluorescence images showing that the mixture of Nephrin-CT, MAGI2, Dendrin, and CD2AP at their individual concentrations of 5 μM or below resulted in condensed droplets with four components codroplet with each other. Nephrin-CT, MAGI2, Dendrin, and CD2AP were labeled with iFluor 405, Cy5, Alexa 488, and Cy3, respectively. Scale bars: 5 μm. (D) Representative SDS-PAGE analysis showing the distributions of wild types (WTs) and mutants of four components in the supernatant (S) and pellet (P) in sedimentation-based assays. The final concentration of each protein was 10 μM. (E) Quantification data of (D). Results are expressed as mean ± SD from three independent batches of sedimentation experiments. IB; immunoblot; PD, pull down; TM, transmembrane.

DISCUSSION

Slit diaphragm is a specialized adhesion junction between the adjacent podocytes. The electron-dense areas located at the cytoplasmic insertion sites of each slit diaphragm have been observed for over 40 years[38] (Figure 6). During the last decades, cell biologic and genetic studies have identified a variety of components (*i.e.*, the slit diaphragm complex) enriched in these protein-rich, semiopen compartments in podocytes, although little is known about how these electron-dense matrixes are assembled. In this work, we discover that MAGI2, a unique member of the MAGUK family scaffold proteins highly expressed at slit diaphragm, can spontaneously undergo LLPS (Figure 1). Driven by the multivalent interactions between MAGI2, Dendrin, and CD2AP, these proteins could form electron-dense matrix-like slit diaphragm condensates. These discoveries suggest that the electron-dense slit diaphragm compartments might form via

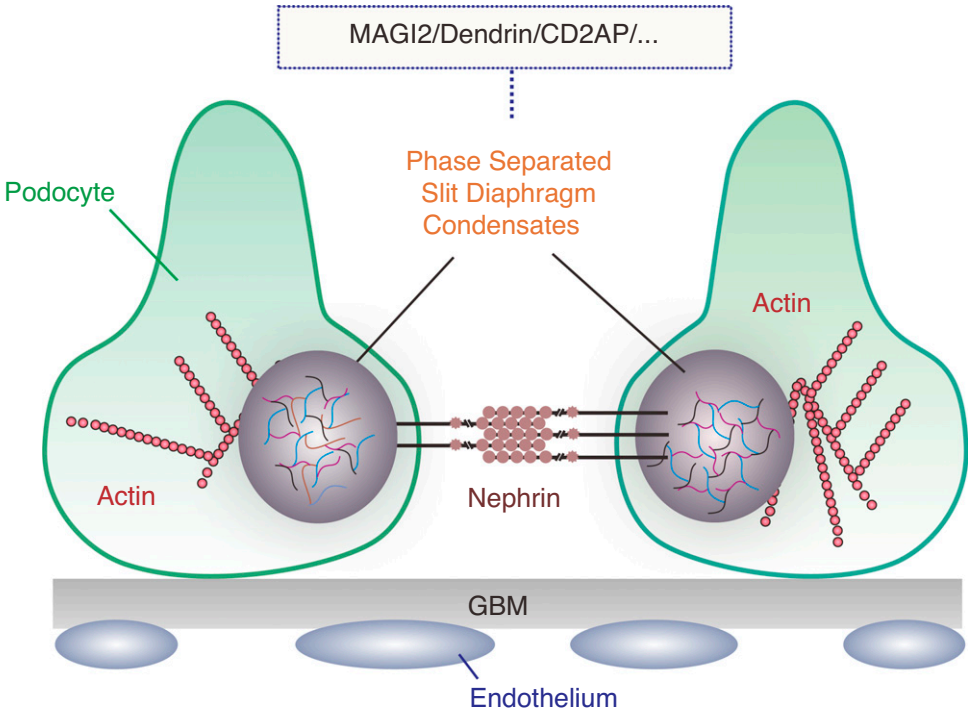

Figure 6. Phase separation-mediated slit diaphragm assembly. Proposed model for slit diaphragm organization mediated by phase separation of the slit diaphragm complex. The slit diaphragm complex including but not limited to the MAGI2-Dendrin-CD2AP axis may autonomously form condensed slit diaphragm condensates in the podocytes via LLPS. The shaded gray spheres indicate that the slit diaphragm condensates could connect slit diaphragm and cortical actin cytoskeleton. GBM, glomerular basement membrane.

phase separation of core components of the slit diaphragm complex (*e.g.*, MAGI2, Dendrin, CD2AP, *etc.*) (Figure 6). Importantly, the reconstituted slit diaphragm condensates could effectively recruit Nephrin. Notably, the condensates composed of Nephrin, MAGI2, Dendrin, and CD2AP could form at their individual concentration of 1 μM, which is close to physiologic concentration. In general, binding of multivalent cognate proteins at the two-dimensional membrane interface has been shown to significantly decrease the threshold concentration for phase separation, as indicated in many systems such as the neuronal synapse,[57] the immunologic synapse,[58] and the tight junction.[59] Consider that other slit diaphragm protein(s) may further expand the valency of the condensates; it would be reasonable to speculate that the slit diaphragm condensates may occur at concentrations even lower than 1 μM. Because CD2AP is a barbed-end capping protein that stabilizes actin filaments,[60] the slit diaphragm condensates are expected to be linked to cortical actin cytoskeleton and strengthen the slit diaphragm architecture in podocytes. Interestingly, a similar mechanism is also applied for formation of the electron-dense junctional plaque at the tight junction in epithelial cells. Phase separation of ZO proteins, which belong to another subfamily of MAGUK scaffold proteins, drives tight junction formation.[59] Tight junction condensates can be enriched in adhesion receptors, cytoskeletal adaptors, and transcription factors.[59] These data together suggested that the electron-dense matrixes observed at cell-cell junctions through transmission electron microscopy may all form via phase separation of core components in these structures.

MAGI1 and MAGI2 are the two major isoforms of MAGI family scaffolds in slit diaphragm, and they play important roles in assembling and maintaining the structural integrity of slit diaphragm. Mutations of *MAGI2* have recently been identified in patients with congenital nephritic syndrome.[31,61] Global and podocyte-specific knockout of *MAGI2* both led to defects in slit diaphragm assembly and massive albuminuria, and the knockout mice died of kidney failure.[32,34] However, the kidneys from the *MAGI1* knockout mice function normally,[62] although the amino acid sequence and overall domain organization between MAGI1 and MAGI2 are extremely similar. These data indicate that some paralog-specific sequences in MAGI2 may be attributed to its critical roles in podocytes. Here, we demonstrate that MAGI2 can autonomously undergo phase separation. Paralog-specific "RQPPxxxDY" repetitive motifs between PDZ4 and PDZ5 domains of MAGI2 are essential for its phase separation, which explains why only MAGI2, but not MAGI1, could form phase-separated condensates. We believe that MAGI2-mediated slit diaphragm condensates

may play crucial roles in slit diaphragm integrity. Although investigation of membrane-attached MAGI2-mediated slit diaphragm condensates in podocytes is still hard to achieve due to technical limits at this stage, future *in vivo* work is definitely needed to demonstrate their critical roles in the glomerular filtration barrier.

In developing glomeruli, Nephrin was phosphorylated upon clustering, which resulted in recruitment of Nck and N-WASP. Interestingly, phosphorylated Nephrin-CT, Nck, and N-WASP together form highly dense condensates via phase separation both in three dimensions and on the model membranes,[63,64] uncovering the molecular mechanism of such Nephrin-dependent signaling in actin polymerization. After the slit diaphragm is assembled, how then is Nephrin tightly connected with the cortical cytoskeleton? Our work provides valuable insights. Nephrin is dephosphorylated as the glomeruli matured[12,15] and might be associated tightly with the cortical actin cytoskeleton via the slit diaphragm condensates formed by the key components, including but not limited to MAGI2-Dendrin-CD2AP complex in the slit diaphragm. In this scenario, two sets of condensates may function during podocyte development and maintenance. Future work is required to investigate how these condensates interplay with each other in podocytes. It should be noted that MAGI2-mediated slit diaphragm condensates should be regulated in order to orchestrate podocyte plasticity. Post-translational modifications by phosphorylation and methylation have been shown to regulate phase separation in many cellular processes.[65,66] Because the tyrosine residues in paralog-specific "RQPPxxxDY" repetitive motifs are crucial for MAGI2 phase separation, phosphorylation at these tyrosine residues might tune the ability of MAGI2 to form phase-separated condensates. It should also be noted that the specific lipid microdomain where Nephrin is embedded definitely plays a critical role in regulation of Nephrin-mediated complex assembly in the mature slit diaphragm.[18,67] Although our data showed that membrane-attached Nephrin-CT did not affect the formation of MAGI2-meidated condensates (Supplemental Figure 8), it is still unknown how the lipid microdomain communicates with the phase separation–mediated membrane-attached condensates to regulate the slit diaphragm assembly.

DISCLOSURES

All authors have nothing to disclose.

FUNDING

This work was supported by National Key R&D Program of China grants 2017YFA0504901 (to R. Zhang) and 2018YFA0507900 (to J. Zhu); National Natural Science Foundation of China grants U2032122 (to J. Zhu) and 31770779 (to J. Zhu); Science and Technology Commission of Shanghai Municipality grant 20S11900200 (to J. Zhu); Research Grants Council, University Grants Committee grants AoE-M09-12 (to M. Zhang) and C6004-17G (to M. Zhang); Shanghai Institutes for Biological Sciences, Chinese Academy of Sciences Chief Scientist Program (to R. Zhang).

ACKNOWLEDGMENTS

We thank the Shanghai Synchrotron Radiation Facility (China) BL17U1, BL18U1, and BL19U1 for x-ray beam time; the staff members of the Large-Scale Protein Preparation System and Molecular Imaging System at the National Facility for Protein Science in Shanghai, Zhangjiang Laboratory, China for providing technical support and assistance in data collection and analysis; and Dr. Wenyu Wen for providing assistance in data collection of fluorescence polarization assay.

H. Zhang and J. Zhu designed the experiments; H. Zhang performed the biochemical experiments; L. Lin, Z. Lin, and H. Zhang carried out the x-ray data collection and structure determination; J. Liu and L. Pan conducted the nuclear magnetic resonance experiments; Y. Cao, H. Zhang, J. Zhang, M. Zhang, R. Zhang, and J. Zhu analyzed the data; J. Zhu drafted the manuscript; J. Zhu coordinated the project; and all authors commented on the manuscript.

DATA AVAILABILITY STATEMENT

The atomic coordinate of the MAGI2-Dendrin complex is deposited in the PDB under the accession code 6KKG.

SUPPLEMENTAL MATERIAL

This article contains the following supplemental material online at http://jasn.asnjournals.org/lookup/suppl/doi:10.1681/ASN.2020111590/-/DCSupplemental.

Supplemental Figure 1. Arginine content of each domain in MAGI2 among different species and MAGI1/3.

Supplemental Figure 2. PDZ5-8RA shows similar binding affinity to δ-catenin PBM with wild-type PDZ5 domain of MAGI2.

Supplemental Figure 3. Amino acid sequence analysis of the SRNS-associated MAGI2 mutation.

Supplemental Figure 4. Mutations interfere with the MAGI2-Dendrin-CD2AP interactions.

Supplemental Figure 5. MAGI2, Dendrin, and CD2AP colocalize with each other in the puncta in cells.

Supplemental Figure 6. A mutant of CD2AP is capable of converting trimeric CD2AP-CC into a monomer.

Supplemental Figure 7. NMR-based titration assays showing that the P1 peptide of CD2AP specifically binds to the SH3 domains of CD2AP.

Supplemental Figure 8. Nephrin-CT, MAGI2, Dendrin, and CD2AP form a complex in vitro and in living cells.

Supplemental Figure 9. Characterization of the bindings of Nephrin-CT to the wild type and nephrotic syndrome–associated mutation of MAGI2.

Supplemental Table 1. X-ray diffraction data collection and refinement statistics.

REFERENCES

1. Greka A, Mundel P: Cell biology and pathology of podocytes. *Annu Rev Physiol* 74: 299–323, 2012
2. Patrakka J, Tryggvason K: Molecular make-up of the glomerular filtration barrier. *Biochem Biophys Res Commun* 396: 164–169, 2010

3. Garg P: A review of podocyte biology. *Am J Nephrol* 47: 3–13, 2018
4. Grahammer F, Schell C, Huber TB: Molecular understanding of the slit diaphragm. *Pediatr Nephrol* 28: 1957–1962, 2013
5. Grahammer F, Schell C, Huber TB: The podocyte slit diaphragm–from a thin grey line to a complex signalling hub. *Nat Rev Nephrol* 9: 587–598, 2013
6. Haraldsson B, Nyström J, Deen WM: Properties of the glomerular barrier and mechanisms of proteinuria. *Physiol Rev* 88: 451–487, 2008
7. Assady S, Wanner N, Skorecki KL, Huber TB: New insights into podocyte biology in glomerular health and disease. *J Am Soc Nephrol* 28: 1707–1715, 2017
8. Conti S, Perico L, Grahammer F, Huber TB: The long journey through renal filtration: New pieces in the puzzle of slit diaphragm architecture. *Curr Opin Nephrol Hypertens* 26: 148–153, 2017
9. Kestilä M, Lenkkeri U, Männikkö M, Lamerdin J, McCready P, Putaala H, et al.: Positionally cloned gene for a novel glomerular protein–nephrin–is mutated in congenital nephrotic syndrome. *Mol Cell* 1: 575–582, 1998
10. Putaala H, Soininen R, Kilpeläinen P, Wartiovaara J, Tryggvason K: The murine nephrin gene is specifically expressed in kidney, brain and pancreas: Inactivation of the gene leads to massive proteinuria and neonatal death. *Hum Mol Genet* 10: 1–8, 2001
11. Lahdenperä J, Kilpeläinen P, Liu XL, Pikkarainen T, Reponen P, Ruotsalainen V, et al.: Clustering-induced tyrosine phosphorylation of nephrin by Src family kinases. *Kidney Int* 64: 404–413, 2003
12. Verma R, Kovari I, Soofi A, Nihalani D, Patrie K, Holzman LB: Nephrin ectodomain engagement results in Src kinase activation, nephrin phosphorylation, Nck recruitment, and actin polymerization. *J Clin Invest* 116: 1346–1359, 2006
13. Jones N, Blasutig IM, Eremina V, Ruston JM, Bladt F, Li H, et al.: Nck adaptor proteins link nephrin to the actin cytoskeleton of kidney podocytes. *Nature* 440: 818–823, 2006
14. Moeller MJ: Dynamics at the slit diaphragm–is nephrin actin'? *Nephrol Dial Transplant* 22: 37–39, 2007
15. Tryggvason K, Pikkarainen T, Patrakka J: Nck links nephrin to actin in kidney podocytes. *Cell* 125: 221–224, 2006
16. Lehtonen S, Ryan JJ, Kudlicka K, Iino N, Zhou H, Farquhar MG: Cell junction-associated proteins IQGAP1, MAGI-2, CASK, spectrins, and alpha-actinin are components of the nephrin multiprotein complex. *Proc Natl Acad Sci U S A* 102: 9814–9819, 2005
17. Fukasawa H, Bornheimer S, Kudlicka K, Farquhar MG: Slit diaphragms contain tight junction proteins. *J Am Soc Nephrol* 20: 1491–1503, 2009
18. Schwarz K, Simons M, Reiser J, Saleem MA, Faul C, Kriz W, et al.: Podocin, a raft-associated component of the glomerular slit diaphragm, interacts with CD2AP and nephrin. *J Clin Invest* 108: 1621–1629, 2001
19. Shih NY, Li J, Cotran R, Mundel P, Miner JH, Shaw AS: CD2AP localizes to the slit diaphragm and binds to nephrin via a novel C-terminal domain. *Am J Pathol* 159: 2303–2308, 2001
20. Asanuma K, Campbell KN, Kim K, Faul C, Mundel P: Nuclear relocation of the nephrin and CD2AP-binding protein dendrin promotes apoptosis of podocytes. *Proc Natl Acad Sci U S A* 104: 10134–10139, 2007
21. Mundel P, Heid HW, Mundel TM, Krüger M, Reiser J, Kriz W: Synaptopodin: An actin-associated protein in telencephalic dendrites and renal podocytes. *J Cell Biol* 139: 193–204, 1997
22. Feng D, DuMontier C, Pollak MR: Mechanical challenges and cytoskeletal impairments in focal segmental glomerulosclerosis. *Am J Physiol Renal Physiol* 314: F921–F925, 2018
23. Subramanian B, Sun H, Yan P, Charoonratana VT, Higgs HN, Wang F, et al.: Mice with mutant Inf2 show impaired podocyte and slit diaphragm integrity in response to protamine-induced kidney injury. *Kidney Int* 90: 363–372, 2016
24. Hirabayashi S, Mori H, Kansaku A, Kurihara H, Sakai T, Shimizu F, et al.: MAGI-1 is a component of the glomerular slit diaphragm that is tightly associated with nephrin. *Lab Invest* 85: 1528–1543, 2005
25. Yamada H, Shirata N, Makino S, Miyake T, Trejo JAO, Yamamoto-Nonaka K, et al.: MAGI-2 orchestrates the localization of backbone proteins in the slit diaphragm of podocytes. *Kidney Int* 99: 382–395, 2021
26. Lehtonen S, Zhao F, Lehtonen E: CD2-associated protein directly interacts with the actin cytoskeleton. *Am J Physiol Renal Physiol* 283: F734–F743, 2002
27. Faul C, Asanuma K, Yanagida-Asanuma E, Kim K, Mundel P: Actin up: Regulation of podocyte structure and function by components of the actin cytoskeleton. *Trends Cell Biol* 17: 428–437, 2007
28. Oh J, Reiser J, Mundel P: Dynamic (re)organization of the podocyte actin cytoskeleton in the nephrotic syndrome. *Pediatr Nephrol* 19: 130–137, 2004
29. Perico L, Conti S, Benigni A, Remuzzi G: Podocyte-actin dynamics in health and disease. *Nat Rev Nephrol* 12: 692–710, 2016
30. Lovric S, Ashraf S, Tan W, Hildebrandt F: Genetic testing in steroid-resistant nephrotic syndrome: When and how? *Nephrol Dial Transplant* 31: 1802–1813, 2016
31. Bierzynska A, Soderquest K, Dean P, Colby E, Rollason R, Jones C, et al.; NephroS; UK study of Nephrotic Syndrome: *MAGI2* mutations cause congenital nephrotic syndrome. *J Am Soc Nephrol* 28: 1614–1621, 2017
32. Ihara K, Asanuma K, Fukuda T, Ohwada S, Yoshida M, Nishimori K: MAGI-2 is critical for the formation and maintenance of the glomerular filtration barrier in mouse kidney. *Am J Pathol* 184: 2699–2708, 2014
33. Balbas MD, Burgess MR, Murali R, Wongvipat J, Skaggs BJ, Mundel P, et al.: MAGI-2 scaffold protein is critical for kidney barrier function. *Proc Natl Acad Sci U S A* 111: 14876–14881, 2014
34. Shirata N, Ihara KI, Yamamoto-Nonaka K, Seki T, Makino SI, Oliva Trejo JA, et al.: Glomerulosclerosis induced by deficiency of membrane-associated guanylate kinase inverted 2 in kidney podocytes. *J Am Soc Nephrol* 28: 2654–2669, 2017
35. Gigante M, Pontrelli P, Montemurno E, Roca L, Aucella F, Penza R, et al.: CD2AP mutations are associated with sporadic nephrotic syndrome and focal segmental glomerulosclerosis (FSGS). *Nephrol Dial Transplant* 24: 1858–1864, 2009
36. Wolf G, Stahl RA: CD2-associated protein and glomerular disease. *Lancet* 362: 1746–1748, 2003
37. Shih NY, Li J, Karpitskii V, Nguyen A, Dustin ML, Kanagawa O, et al.: Congenital nephrotic syndrome in mice lacking CD2-associated protein. *Science* 286: 312–315, 1999
38. Schneeberger EE, Levey RH, McCluskey RT, Karnovsky MJ: The isoporous substructure of the human glomerular slit diaphragm. *Kidney Int* 8: 48–52, 1975
39. Mundel P, Kriz W: Structure and function of podocytes: An update. *Anat Embryol (Berl)* 192: 385–397, 1995
40. Ichimura K, Sakai T: Evolutionary morphology of podocytes and primary urine-producing apparatus. *Anat Sci Int* 92: 161–172, 2017
41. Minor W, Cymborowski M, Otwinowski Z, Chruszcz M: HKL-3000: The integration of data reduction and structure solution–from diffraction images to an initial model in minutes. *Acta Crystallogr D Biol Crystallogr* 62: 859–866, 2006
42. McCoy AJ, Grosse-Kunstleve RW, Adams PD, Winn MD, Storoni LC, Read RJ: Phaser crystallographic software. *J Appl Cryst* 40: 658–674, 2007
43. Adams PD, Afonine PV, Bunkóczi G, Chen VB, Davis IW, Echols N, et al.: PHENIX: A comprehensive Python-based system for macromolecular structure solution. *Acta Crystallogr D Biol Crystallogr* 66: 213–221, 2010
44. Emsley P, Cowtan K: Coot: Model-building tools for molecular graphics. *Acta Crystallogr D Biol Crystallogr* 60: 2126–2132, 2004

45. Weng Z, Shang Y, Ji Z, Ye F, Lin L, Zhang R, et al.: Structural basis of highly specific interaction between Nephrin and MAGI1 in slit diaphragm assembly and signaling. *J Am Soc Nephrol* 29: 2362–2371, 2018
46. Hyman AA, Weber CA, Jülicher F: Liquid-liquid phase separation in biology. *Annu Rev Cell Dev Biol* 30: 39–58, 2014
47. Banani SF, Lee HO, Hyman AA, Rosen MK: Biomolecular condensates: Organizers of cellular biochemistry. *Nat Rev Mol Cell Biol* 18: 285–298, 2017
48. Shin Y, Brangwynne CP: Liquid phase condensation in cell physiology and disease. *Science* 357: eaaf4382, 2017
49. Murthy AC, Dignon GL, Kan Y, Zerze GH, Parekh SH, Mittal J, et al.: Molecular interactions underlying liquid-liquid phase separation of the FUS low-complexity domain. *Nat Struct Mol Biol* 26: 637–648, 2019
50. Dosztányi Z, Csizmok V, Tompa P, Simon I: IUPred: Web server for the prediction of intrinsically unstructured regions of proteins based on estimated energy content. *Bioinformatics* 21: 3433–3434, 2005
51. Wang J, Choi JM, Holehouse AS, Lee HO, Zhang X, Jahnel M, et al.: A molecular grammar governing the driving forces for phase separation of prion-like RNA binding proteins. *Cell* 174: 688–699.e16, 2018
52. Salah Z, Alian A, Aqeilan RI: WW domain-containing proteins: Retrospectives and the future. *Front Biosci* 17: 331–348, 2012
53. Lin Z, Yang Z, Xie R, Ji Z, Guan K, Zhang M: Decoding WW domain tandem-mediated target recognitions in tissue growth and cell polarity. *eLife* 8: e49439, 2019
54. Li Q, Yang W, Wang Y, Liu W: Biochemical and structural studies of the interaction between ARAP1 and CIN85. *Biochemistry* 57: 2132–2139, 2018
55. Kühn J, Wong LE, Pirkuliyeva S, Schulz K, Schwiegk C, Fünfgeld KG, et al.: The adaptor protein CIN85 assembles intracellular signaling clusters for B cell activation. *Sci Signal* 9: ra66, 2016
56. Zeng M, Shang Y, Araki Y, Guo T, Huganir RL, Zhang M: Phase transition in postsynaptic densities underlies formation of synaptic complexes and synaptic plasticity. *Cell* 166: 1163–1175.e12, 2016
57. Zeng M, Chen X, Guan D, Xu J, Wu H, Tong P, et al.: Reconstituted postsynaptic density as a molecular platform for understanding synapse formation and plasticity. *Cell* 174: 1172–1187.e16, 2018
58. Su X, Ditlev JA, Hui E, Xing W, Banjade S, Okrut J, et al.: Phase separation of signaling molecules promotes T cell receptor signal transduction. *Science* 352: 595–599, 2016
59. Beutel O, Maraspini R, Pombo-García K, Martin-Lemaitre C, Honigmann A: Phase separation of zonula occludens proteins drives formation of tight junctions. *Cell* 179: 923–936.e11, 2019
60. Tang VW, Brieher WM: FSGS3/CD2AP is a barbed-end capping protein that stabilizes actin and strengthens adherens junctions. *J Cell Biol* 203: 815–833, 2013
61. Ashraf S, Kudo H, Rao J, Kikuchi A, Widmeier E, Lawson JA, et al.: Mutations in six nephrosis genes delineate a pathogenic pathway amenable to treatment. *Nat Commun* 9: 1960, 2018
62. Ni J, Bao S, Johnson RI, Zhu B, Li J, Vadaparampil J, et al.: MAGI-1 interacts with Nephrin to maintain slit diaphragm structure through enhanced Rap1 activation in podocytes. *J Biol Chem* 291: 24406–24417, 2016
63. Li P, Banjade S, Cheng HC, Kim S, Chen B, Guo L, et al.: Phase transitions in the assembly of multivalent signalling proteins. *Nature* 483: 336–340, 2012
64. Banjade S, Rosen MK: Phase transitions of multivalent proteins can promote clustering of membrane receptors. *eLife* 3: e04123, 2014
65. Tsang B, Arsenault J, Vernon RM, Lin H, Sonenberg N, Wang LY, et al.: Phosphoregulated FMRP phase separation models activity-dependent translation through bidirectional control of mRNA granule formation. *Proc Natl Acad Sci U S A* 116: 4218–4227, 2019
66. Kim TH, Tsang B, Vernon RM, Sonenberg N, Kay LE, Forman-Kay JD: Phospho-dependent phase separation of FMRP and CAPRIN1 recapitulates regulation of translation and deadenylation. *Science* 365: 825–829, 2019
67. Huber TB, Simons M, Hartleben B, Sernetz L, Schmidts M, Gundlach E, et al.: Molecular basis of the functional podocin-nephrin complex: Mutations in the NPHS2 gene disrupt nephrin targeting to lipid raft microdomains. *Hum Mol Genet* 12: 3397–3405, 2003

AFFILIATIONS

[1]State Key Laboratory of Cell Biology, Shanghai Institute of Biochemistry and Cell Biology, Chinese Academy of Sciences Center for Excellence in Molecular Cell Science, Chinese Academy of Sciences, University of Chinese Academy of Sciences, Shanghai, China
[2]Bio-X Institutes, Key Laboratory for the Genetics of Developmental and Neuropsychiatric Disorders, Ministry of Education, Shanghai Jiao Tong University, Shanghai, China
[3]State Key Laboratory of Bioorganic and Natural Products Chemistry, Center for Excellence in Molecular Synthesis, Shanghai Institute of Organic Chemistry, University of Chinese Academy of Sciences, Chinese Academy of Sciences, Shanghai, China
[4]Division of Life Science, State Key Laboratory of Molecular Neuroscience, Hong Kong University of Science and Technology, Clear Water Bay, Kowloon, Hong Kong, China
[5]School of Life Sciences, Southern University of Science and Technology, Shenzhen, China
[6]School of Life Sciences and Technology, Tongji University, Shanghai, China